Microphase Separation of Bulk and Ultrathin Films of Polyurethane Elastomers

Mutsuhisa Furukawa,[*1] *Ken Kojio,*[2] *So Kugumiya,*[1] *Yusuke Uchiba,*[1] *Yoshitaka Mitsui*[1]

Surmmary: Polyurethane elastomers (PUEs) were synthesized with poly(oxytetramethylene) glycol (PTMG), 4,4′-diphenylmethane diisocyanate (MDI) and 1,4-butanediol (BD)/1,1,1-trimethylol propane (TMP) by a prepolymer method. The degree of microphase separation of bulk and ultrathin films for these PUEs was confirmed by Fourier transform infrared (FT-IR) spectroscopy, differential scanning calorimetry (DSC) and atomic force microscopy (AFM). In the bulk films, FT-IR and DSC measurements revealed that the degree of micro-phase separation strengthened with increasing BD content. AFM observation of the BD-PUE showed hard segment domains surrounded by a soft segment matrix. The domains ranged in size from 10-20 nm, while BD/TMP- and TMP PUEs did not have clear domains. On the other hand, AFM observation was carried out on thin films (200 mm in thickness) and ultrathin films (approximately 8-5 nm) prepared by spin-coating the different concentrations of PUE solutions. The microphase separated strucuture under 10 nm in thickness showed marked decreases in the size of the microphase-separated domain.

Keywords: AFM; DSC; FT-IR; microstructure; polyurethanes

Introduction

Polyurethane elastomers (PUEs) have excellent mechanical properties and biocompatiblity.[1–16] It is well known that these excellent properties arise from the microphase-separated structure. The microphase-separated structures of PUEs have been clarified by applying small angle x-ray scattering (SAXS)[10,11] and transmission electron microscopy (TEM). Atomic force microscopy (AFM) is a very powerful tool for direct observation of microphase separation.[12–16] In this study, microphase-separated structures of bulk PUEs and their corresponding ultrathin films, prepared from PTMG, MDI and BD, or BD/TMP, were directly observed using AFM. Microphase separation was confirmed by Fourier transform infrared (FT-IR) spectroscopy, differential scanning calorimetry (DSC) and AFM.

Experimental Part

Materials

Poly(oxytetramethylene) glycol (PTMG: $M_n =$ 2000, Asahikasei Chemicals Co., Ltd., Japan), 4,4′-diphenylmethane diisocyanate (MDI, Nippon Polyurethane Industry Co., Ltd., Japan) and 1,4-butandiol (BD) and 1,1,1-trimethylol propane (TMP, Wako Chemicals Co., Ltd., Japan) were used. The curing agents used to control the microphase separation were BD, TMP and a mixture of BD plus TMP at weight ratio of 75/25.

[1] Department of Materials Science, Graduate School of Science and Technology, Nagasaki University, 1-14 Bunkyo-machi, Nagasaki 852-8521, Japan
E-mail: furukawa@nagasaki-u.ac.jp
[2] Department of Materials Science and Engineering, Faculty of Engineering, Nagasaki University, 1-14 Bunkyo-machi, Nagasaki 852-8521, Japan

Synthesis of Polyurethane Elastomers

The PUEs were synthesizsed by a bulk prepolymer method at the ratio of K = [NCO]/[OH] = 3.30 and NCO Index = 1.05 under a nitrogen atmosphere. For AMF observation of the bulk PUEs, the PUE sheets were sliced. Each cross section was then fixed on a silicon wafer substrate. In contrast, for the ultrathin film PUEs, a different terahydrofuran concentration of BD-PUE solution was spin-casted on a silicon wafer. The thin PUE films were prepared on a silicon wafer from the tetrahydrofuran PUE solution by a spin coating method. Then, the samples were dried under a vacuum to remove residual solvent. Film thickness was controlled by changing the solution concentration.

Charactrization

FT-IR spectra were obtained with an FTS-3000 EXCALIBUR (Digilab Japan Co., Ltd. Japan) equipped with an MCT detector using an ATR cell (MIR., PIK). XPS measurement was carried out to analyze the surface chemical composition of the PU films. PHI 5800 with a monochromated x-ray source was employed. The emission angles were 75° and 30°, with corresponding analytical depths of 10.1 and 5.3 nm. Microphase-separated structures of the PU films were observed by AFM using a Seiko Instrument. Since PU includes the rubbery soft segments at room temperature, we applied an intermittent mode for the observation. Both topography and phase images were collected. To avoid destruction of the sample surface, the images were acquired under ambient conditions using light to moderate tapping, r = 0.90–0.80, where r = (set point amplitude/free amplitude of oscillation). Cantilevers employed were SI-DF-20 with a spring constant of 14 N m^{-1} and a resonance frequency of 130 kHz.

The domain spacing of the microphase-separated structure in the PUE films was investigated based on grazing incident small angle X-ray scattering (GISAXS) measurement. These measurements were carried out at the BL40 beam line in the Syncrotron radiation facility, Spring-8. The incident angle and exposure time were 0.15 and 60 sec, respectively. In order to assure the sensitivity of the CCD camera, the beam stopper was placed along the azimuthal direction. Since the GISAXS patterns are obtained utilizing reflected x-ray beams, the scattered light is observed on the Yoneda line. All samples clearly exhibited broader peaks along the in-plane direction. To discuss the peak position in the q direction, intensity vs q profiles were obtained by integration along the Yoneda line.

Results and Discussion

Effects of Curing Agents on Microphase Separation

Different microphase separated PUEs were prepared by changing the mixing ratio of BD to TMP as a curing agent. The microphase seprated strucures of these PUEs were observed using AFM in addition to FT-IR, DSC and SAXS. Figure 1 shows the FT-IR spectra of the PUEs used. Hydrogen bonded NH groups with ether oxygen ($\nu_{NHether}$) and urethane carbonyl oxygen ($\nu_{NHcarbonyl}$) were observed at 3290–3310 and 3300–3350 cm^{-1}, respectively. These results indicate that all NH groups hydrogen bonded with ether or urethane carbonyl groups. For the C=O stretching bands ($\nu_{C=O}$), two peaks were observed at approximately 1704 and 1730 cm^{-1}, which can be assigned to the hydrogen bonded carbonyl stretching bond ($\nu_{C=O\ H\text{-}bond}$)) and the free bond ($\nu_{C=O\ free}$). The intensity ratio of the $\nu_{C=O\ H\text{-}bond}$ to the $\nu_{C=O\ free}$ increased as the TMP content decreased, indicating the ordered aggregation of the hard segment chains to be progressive for the BD PUE.

Figure 2 shows DSC thermograms of PUEs. The glass transition temperature (T_g) and the melting temperature of the soft segment chains for the BD were observed around -70 and 7 °C. T_g of the soft segment chains increased with TMP content. In contrast, the melting point of the hard

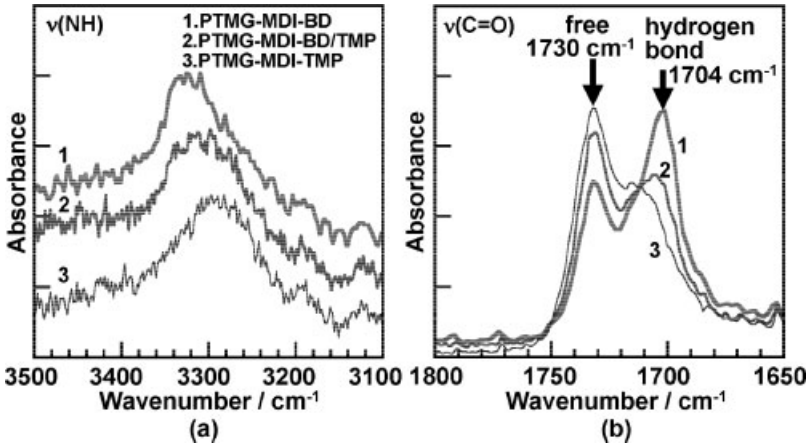

Figure 1.
FT-IR spectra of PTMG-MDI-BD, BD/TMP and TMP. (a) NH streching band, (b) C=O streching band reagion.

segment domains was observed to be approximately 160 °C for the BD PUE which decreased as the TMP content increased. Both the FT-IR and the DSC data clearly indicate that the degree of microphase separation strengthens as the hard segment content decreases.

Figure 3 shows the AFM phase images of the BD, BD/TMP and TMP PUEs. Brighter and darker portions of the phase images correspond to larger phase lags. Isolated small relatively dark dots were clearly observed in BD PUE, while these dots were not seen with the BD/TMP and TMP PUEs. Thus, the isolated hard segment domains were surrounded by a soft segment matrix in the BD PUE. The interdomain spacing, as estimated from these data, was 22.6 nm. The peak of the SAXS profile for the BD PUE was observed at 0.42 nm^{-1}, and the inter-domain spacing was approximately 16 nm. Segment domains with sizes corresponding well to the results obtained from SAXS were initially observed. These results show that segmented polyurethanes are nanocomposites consisting of hard domains, as a reinforced filler, and soft domains, as an elastic matrix.

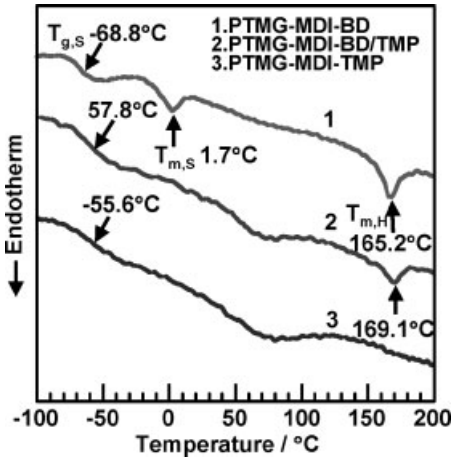

Figure 2.
DSC thermograms of PTMG-MDI based PUEs cured with BD, BD/TMP and TMP.

Comparison the Microphase Separation of Ultrathin Film from Thin Film

It is anticipated that strong polar groups would facilitate the formation of a stable film even at the molecular level and strongly affect the microstructure of polymer ultrathin films. As described above, PTMG-MDI-BD bulk films undergo microphase separation at the nanometer level. In order to confirm the effects of the urethane groups on the microstrucuture of polyurethane ultrathin films, the surface chemical compositions of thin PUE films with diffrent thicknesses were studied using

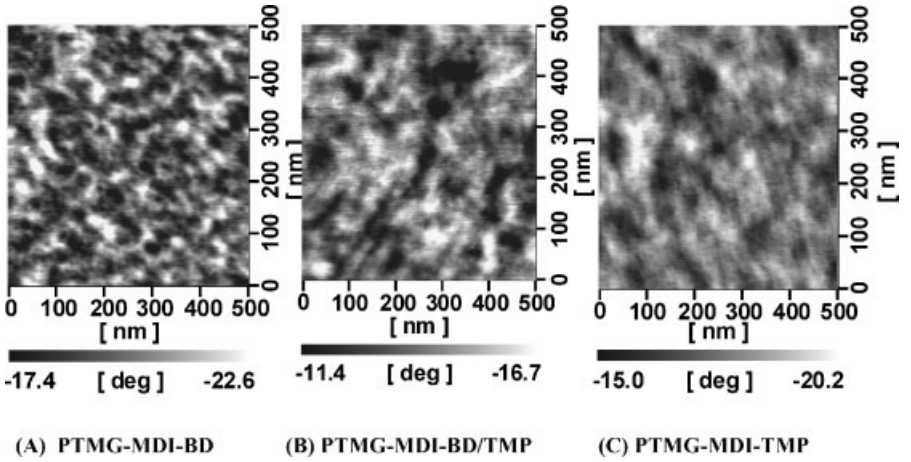

Figure 3.
AFM phase images of (a) PTMG-MDI-BD (HSC = 34wt%), (b) PTMG-MDI-BD/TMP and (c) PTMG-MDI-TMP.

XPS. Figure 4 shows the XPS C_{1s} spectra for thin films with thicknesses of 200 and 7 nm. The peaks observed at 284.8, 286.5 and 288.0 eV can be assigned to neutral carbon (C–C*–C), ether carbon (C*–O) and urethane carbonyl carbon (NH-C*(=O)–O), respectively. The peak intensities of NH–C*(=O)–O and C*–O for the 7 nm in thickness film were larger and smaller than those for the 200 nm film. This result indicates that the lower surface free energy component, PTMG, was slightly decreased on the upper surface for ultrathin film. However, since the NH–C*(=O)–O peak was clearly observed for the thicker film even at an emission angle of 30°, the surface was not completely covered with the PTMG layer, at least in the 5 nm region. This is due mainly to the multiblock structure, the block sequence of which is smaller than 5 nm in the extended state. In other words, preferential surface segregation barely occurs for polyurethane films. Figure 5 shows the film thickness dependence of the intensity ratio of urethane carbonyl carbon, to ether carbon ([NH–C*(=O)–O]/[C*–O]), for the thin PU films. The magnitudes of [NH–C*(=O)–O]/[C*–O] at greater analytical depths (open symbols) were larger than at lesser analytical

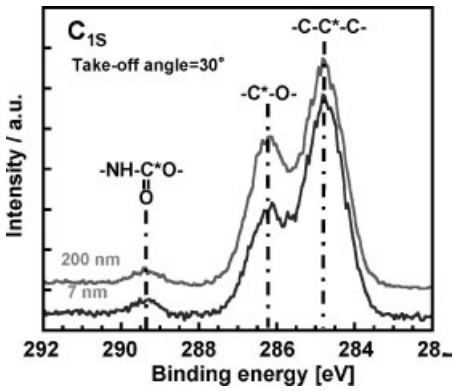

Figure 4.
XPS C_{1s} spectra of PTMG-MDI-BD.

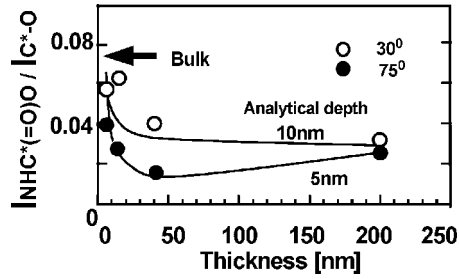

Figure 5.
Film thickness dependence of the intensity ratio of [NH–C*(=O)–O]/[C*–O].

depths (filled symbols), indicating PTMG enrichment on the upper surface. It is intriguing that the magnitude increased as the film thickness decreased to approximately 10 nm. Since these results imply that the enrichment of the PTMG component on the upper surface had disappeared, the chain and/or microphase-separated structure might have changed at a thickness of less than 10 nm.

Figure 6 shows the thickness dependence of the intensity ratio of the (ν(C=Ofree) peak to the (ν(C=OH-bond) peak. The magnitude of $I\nu(C{=}O_{free})/I\nu(C{=}O_{H\text{-}bond})$ in the FT-IR spectra for the films became larger than with a film thickness of only approximately 10 nm. This appears to indicate that the chain structure below 10 nm in thickness generally differs from that of thicker films. These results show that the transition moment of the carbonyl stretching band is perpendicular to the molecular axis. Thus, our experimental results indicate that the hard segment chains with free carbonyl groups were strongly attached to the film/substrate interface oriented in parallel to the interface with decreasing film thickness. Since the hard segment chains have strong polar groups, it is reasonable to speculate that the free hard segment chains are preferentially stacked onto the hydrophilic substrate surface with hydroxyl groups.

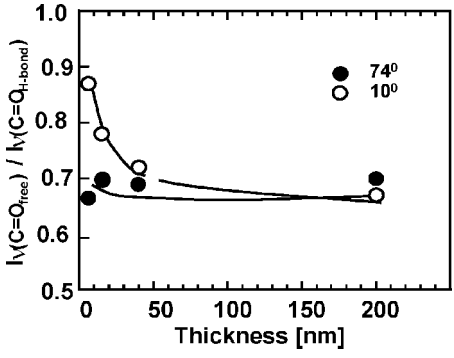

Figure 6.
Thickness dependence of intensity ratio of (ν(C=O_{free}) peak to (ν(C=$O_{H\text{-}bond}$) peak.

Figure 7 shows the AFM phase images of the BD films with thicknesses of 200, 40, 20 and 6 nm. The brighter portion corresponds to the larger phase lag region. It is quite difficult to interpret the phase images because they result from various factors, for example, surface elasticity, adhesion force and so on. As for the occupied area, it is reasonable to speculate that the darker domains and brighter matrix correspond to the hard and soft segments, respectively. The microphase-separated structure for a film thickness of 200 nm was similar to that of the bulk film, as shown in Figure 3(a). The sizes of the microphase-separated structures appear to differ depending on film thickness, that is, the sizes of domains decreased as the film thickness decreased. The microphase-separated domains were smaller at a thickness of 20 or 6 nm. The GISAXS pattern peaks assigned to domain spacing for films with various thicknesses were clearly observed, as shwon in Figure 8. These peak positions shifted to the high q range as film thickness decreased to less than 15 nm. Figure 9 shows the film thickness dependence of domain spacing for the BD films. Domain spacing abruptly decreased as the film thickness decreased. The domain spacings for thicker and thinner films of the BD PUE were 24 and 20 nm, respectively. These trends were all essentially the same as those obtained with AFM. The hard segment chains, -(MDI-BD)$_n$-, of the PU used in this study possess a high degree of crystallizability. Thus, the formation mechanism of the microphase-separated structure of the PUE is closely related to the crystallization of the hard segment chains. As the film thickness decreases, the space for crystallization of the hard segment chains diminishes. Thus, there is not enough space for crystallization of the hard segment chains for the thinner films. Therefore, these reductions in domain size are thought to simply invovle the relationship between space and domain size. With decreasing film thickness, the microphase separated domains decrease in size, as clarified by AFM and GISAXS, resulting in the interfacial region, between

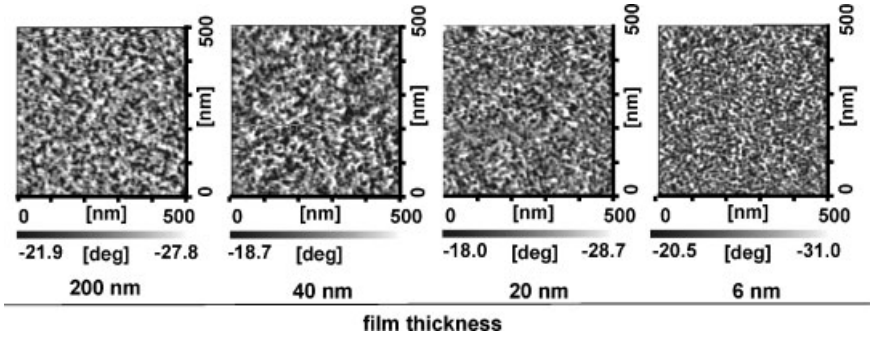

Figure 7.
The AFM phase images of the PU films with different thickness.

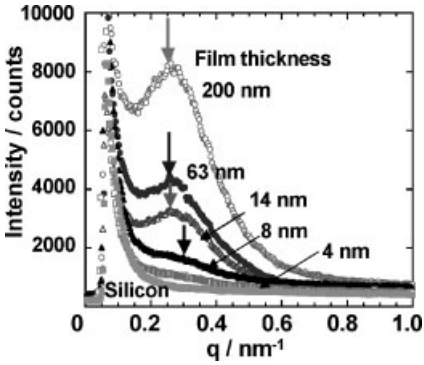

Figure 8.
Thickness dependence of intensity ratio of (ν(C=O$_{free}$) peak to (ν(C=O$_{H\text{-}bond}$) peak.

the hard segment domains and soft segment matrix, increasing. The degree of aggregation of the hard segment chains at the interface might be looser than for hard segment domains. Thus, it is reasonable to speculate that aggregation of the hard segment chains weakens with decreasing film thickness, as shown by FT-IR.

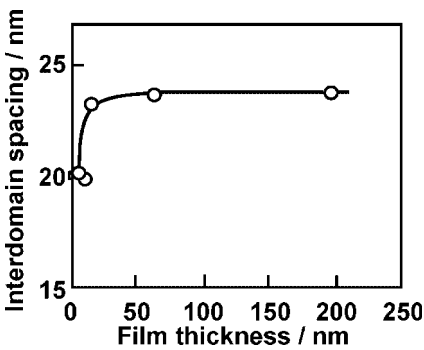

Figure 9.
Film thickness dependence of domain spacing for the PTMG-MDI-BD.

Conclusions

Microphase separation structures of PTMG-MDI-BD, BD/TMP and TMP PUEs were confirmed by FT-IR, DSC, SAXS and AFM. The degree of micro-phase separation strengthened as the TMP content increased. AFM observation for BD PUE showed hard segment domains to be surrounded by a soft segment matrix with an inter-domain size of 22 nm. These results suggest that segmented polyurethanes are nanocomposites consisting of hard domains, as a reinforced filler, and soft domains, as an elastic matrix.

Film thickness dependence of the microphase sepration structure for PTMG-MDI-BD was also studied. The microphase-separated domain decreased in size as film thickness decreased. Inter-domain spacing drastically decreased, from 24 nm to 20 nm, at an ultrathin film thickness of 10 nm, that is, microphase-separated domain size was diminished. This contributed to the strong interaction between the PU films and the substrate surface.

Acknowledgements: The authors are thankful to Dr. S. Sasaki (JASRI), Dr. H. Matsunaga (JASRI) and Dr. H. Okuda (Kyoto University) for the GISAXS measurements and discussion.

[1] H. N. Ng, A. E. Allegrezza, R. W. Seymour, S. L. Cooper, *Polymer* **1972**, *14*, 255.
[2] M. Furukawa, M. Komiyama, T. Yokoyama, *Angew. Makro. Chem.* **1996**, *240*, 205.
[3] T. Okazaki, M. Furukawa, T. Yokoyama, *Polymer J.* **1997**, *29*, 617.
[4] K. Kojio, T. Fukumaru, M. Furukawa, *Macromolecules* **2004**, *37*, 3287.
[5] K. Kojio, Y. Nonaka, M. Furukawa, *J. Polym. Sci. Polym. B. Phys. Edn.* **2004**, *42*, 4448.
[6] K. Kojio, S. Nakamura, M. Furukawa, *Polymer* **2004**, *45*, 8147.
[7] M. Furukawa, Y. Mitsui, T. Fukumaru, K. Kojio, *Polymer* **2005**, *46*, 10817–10822.
[8] S. Yamasaki, D. Nishiguchi, K. Kojio, M. Furukawa, *J. Polym. Sci., Polym. Phys.* **2007**, *45*, 800–814.
[9] K. Kojio, S. Nakashima, M. Furukawa, *Polymer* **2007**, *48*, 997–1004.
[10] J. T. Koberstein, R. S. Stein, *J. Polym. Sci. Polym. Phys.* **1983**, *21*, 1439–1472.
[11] J. T. Koberstein, T. P. Russell, *Macromolecules* **1986**, *19*, 714.
[12] R. S. McLean, B. B. Sauer, *Macromolecules* **1997**, *30*, 8314–8317.
[13] J. T. Garrett, J. Runt, J. S. Lin, *Macromolecules* **2000**, *33*, 6353–6359.
[14] J. T. Garrett, C. A. Siedlecki, J. Runt, *Macromolecules* **2001**, *34*, 7066–7070.
[15] A. Aneja, G. L. Wilkes, *Polymer* **2003**, *44*, 7221–7228.
[16] K. Kojio, Y. Uchiba, Y. Mitsui, M. Furukawa, S. Sasaki, H. Matsunaga, H. Okuda, *Macromolecules* **2007**, *40*, 2625–2628.

